Determination of a Tyre's Rolling Resistance Using Parallel Rheological Framework

Aldhufairi, Hamad; Olatunbosun, Remi; Essa, Khamis

DOI:
10.4271/2019-01-5069

Document Version
Peer reviewed version

Citation for published version (Harvard):
Aldhufairi, H, Olatunbosun, R & Essa, K 2019, 'Determination of a Tyre's Rolling Resistance Using Parallel Rheological Framework', *SAE Technical Paper*, vol. 2019-January, no. January, 2019-01-5069. https://doi.org/10.4271/2019-01-5069

Determination of Tire's Rolling Resistance using Parallel Rheological Framework

Hamad Sarhan Aldhufairi[1], Oluremi Ayotunde Olatunbosun[1] and Khamis Essa[1]

[1] University of Birmingham, Department of Mechanical Engineering, Birmingham, B15 2TT, UK

Abstract

Nowadays, rolling-resistance sits at the core of tire development goals because of its considerable effect on the car's fuel economy. In contrast to the experimental method, the finite element (FE) method offers an inexpensive and efficient estimation technique. However, the FE technique is yet to be a fully developed product particularly for rolling-resistance estimation. An assessment is conducted to study the role of material viscoelasticity representation in FE, in linear and non-linear forms, through using Prony series and parallel rheological framework (PRF) models respectively on the tire's rolling-resistance calculation and its accuracy. A unique approach was introduced to estimate the rolling-resistance according to the tire's hysteresis energy coefficient. The non-linear PRF choice showed rolling-resistance calculations that reasonably match that of the experimental work and the literature for various vertical load and inflation cases, whereas Prony series option was found irresponsive to the tire's deformation in which it gave unreliable and infinitesimal outputs.

Introduction

Primarily, rolling-resistance is seen as the mechanical energy losses, in terms of heat dissipation, incurred as a result of tire deformation while rolling. These losses can reach up to 30% of vehicle fuel usage depending on the driving route [1-4]. In a straight free-rolling condition on a flat surface, a core contributor to the tire's rolling-resistance is the mechanical hysteresis of the tire's structure induced by the material viscoelasticity which can represent up to 95% of rolling-resistance while minor contributors like road-slip and aerodynamic drag can account for up to around 5% and 15% respectively [3, 5-9].

Many efforts have been exerted to capture the tire's viscoelasticity response to compute rolling-resistance via FE approach as a cost-saving alternative to the expensive experimental approach [10, 11]. Various solutions were adopted to calculate the rolling-resistance in terms of "resistive force" or "energy consumed per unit distance travelled" where the second definition (i.e. energy consumption) is commonly utilised since it provides a more complete and appropriate measure [12-15]. Generally, the energy lost in a tire is estimated in FEA by using either an "in-house post FE code based on a viscoelastic theory" or a "built-in viscoelastic function available in the given FE solver" [16].

For the "viscoelastic theory code", commonly, an in-house code is used as a post-processing analyser of the stress-strain time outputs of an FE solver and the material loss coefficients obtained experimentally to calculate the rolling-resistance as per the viscoelastic theory which was written in the code. This methodology is applied by a lot of researchers such as Hoever [12], Ghosh [14] and Cho *et al.* [17]. Most of the presented works use a viscoelastic theory code that is built for in-house application and not for public use [11, 18-22]. Also, commonly, the code would include linear viscoelastic based assumptions to solve the tire's dynamical behaviour which is, however, highly non-linear, thus undermining the calculation accuracy [23]. In addition, the code is normally linked with FE model(s) of quasi-static contact and not compatible with dynamical contact model(s) as it would require way much lengthier and very complicated written code(s) [11, 16].

For the "FE solver built-in functions", most FE solvers employ linear viscoelastic functions to describe the highly non-linear tire behavior [23, 24]. Examples of this are the investigations carried out by Hernandez *et al.* [25], Ghosh *et al.* [16] and Kim *et al.* [26]. These functions rely on the type of experimental material data used for fitting them in terms of the sort of material deformation, strain level(s), and/or response patterns under which the data were obtained. This has limited the validity of those functions and their implementation scope [16]. Furthermore, there is the trade-off between the calculation precision, the model complexity and the resources usage [11, 25].

Based on the earlier findings, the FE option is found to require yet more improvements, when it comes to rolling-resistance modelling, to address its computational inaccuracies in establishing the sophisticated non-linear relationship between the structural hysteresis and the rolling-resistance which is more complicated with the involvement of the operational settings and the geometrical non-linearity [11, 27].

In this regard, this paper reports on the potential for implementing the non-linear viscoelastic PRF model as a more reliable replacement of the classical linear Prony series in FE approach for estimating the rolling-resistance due to the mechanical hysteresis in the tire structure only. The paper's scope excludes other factors of minor contribution to rolling-resistance like aerodynamic-drag and road surface. This is because this paper's goal is to develop an FE model capable of simulating the tire structural effects alone on the tire's rolling-resistance as a part of future work to investigate tire structural design related to tire designing and prototyping. The FE option is found as an emerging solution that is time-saving, cost-effective, easy-to-implement and modifiable compared to the costly, time-consuming, lengthy, hard-to-implement and irreversible experimental option with little gains in general [11, 12, 14, 25, 27-30]. In this context, this paper contributes to increasing the reliability and effectiveness of the

FE solution by introducing a working FE model that can serve as an initial and in-depth evaluation tool of the effect of tire structural design on rolling-resistance at a very early stage of the design process saving a lot of time and costs in narrowing down the potential tire designs for low rolling-resistance. Furthermore, the FE model presented in this paper can be used as a guide and a starting platform toward developing more advanced FE modelling of tire for more complicated or tailored applications.

For this study, the rolling-resistance calculation is performed based on a proposed method that uses the tire's energy dissipation ratio. Abaqus/Explicit was employed to build a complete FE tire model, simulate the tire's free-rolling, and obtain the related energy results to estimate the rolling-resistance. The FE outputs of the tire's rolling-resistance using PRF and Prony series functions, respectively, were compared with the equivalent experimental results to validate both FE methodologies.

Material Characteristics

A 225/55 R17 tire was adopted for the analysis. To predict the rolling behaviour of the tire in FE, the hyperelasticity and viscoelasticity of the tire's rubber components, besides the elasticity of the tire's reinforcements, were necessary [31, 32].

Hyperelasticity Property

To simulate the elastic behaviour of the tire's rubbers, the hyperelastic property was acquired from the stress-strain records measured by performing a uniaxial tensile experiment, as per ASTM D412−15a [33], for the relevant tire's rubber parts. These are the tread, sidewall and chafer/apex. In addition, the rubber's behaviour is taken to be isotropic and almost incompressible.

A least squares data fitting was performed via Abaqus 6.13 to fit the candidate hyperelastic functions (i.e. Arruda Boyce, Ogden, Mooney Rivlin, Neo Hooke and Yeoh) to the experimental test data in order to identify the best fit function to simulate the tire's hyperelasticity. Based on the fitting in Figure 1 and Drucker stability criterion in Abaqus [34], Yeoh was selected to be the best hyperelastic function for the FE tire model since it showed a close fit, demonstrated compatibility with various deformational types, and required affordable experimental work for material property capture. For the other hyperelastic functions, compared to Yeoh, they had either a bad fit to the test data as seen in Figure 1 or were unstable under different deformational modes, according to Drucker stability criterion in Abaqus, which makes them inadequate given the complexity and diversity of tire deformation during rolling. Such an example would be the Ogden function which had the best fit among all other functions but was highly unstable under tension and compression modes whether uniaxially, biaxially, or planarly. The selected Yeoh hyperelastic function used in Abaqus is given in Eq. (1) [34]:

$$U = C_{10}(\bar{I}_1 - 3) + C_{20}(\bar{I}_1 - 3)^2 + C_{30}(\bar{I}_1 - 3)^3 + \cdots + \frac{1}{D_1}(J^{el} - 1)^2 + \frac{1}{D_2}(J^{el} - 1)^4 + \frac{1}{D_3}(J^{el} - 1)^6 \quad (1)$$

Where,
U = Strain Energy per Unit of Reference Volume.
C_{i0} and D_i = Material Parameters.
$\bar{I}_1$ = First Deviatoric Strain Invariant.
J^{el} = Elastic Volumetric Ratio.

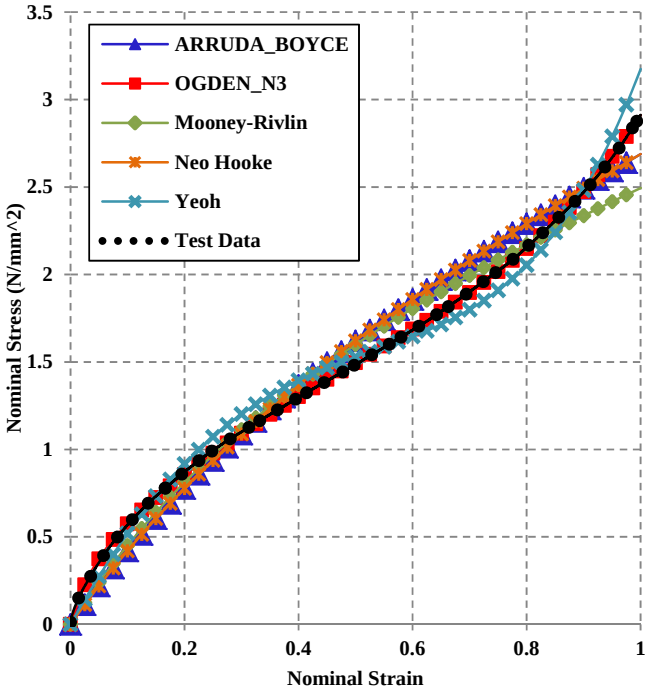

Figure 1. Hyperelastic Functions Fitting for Tread Sample.

The material coefficients (C_{i0}) which were determined using the data fitting procedure in Abaqus, and used for Yeoh function characterisation, are as follows:

Table 1. Yeoh Function Constants for Tire Components.

Yeoh Parameters	Tire Components		
	Tread	Sidewall	Apex
C10	1.0	0.5	1.6
C20	-0.3	-0.1	-1.4
C30	0.1	0.03	0.9

Linear Viscoelasticity Property

In Abaqus, the FE solver offers extraction of rubber viscoelasticity in the linear form through the Prony series function. The Prony series function was fitted to represent the linear viscoelasticity of the different tire rubber parts based on the stress relaxation experimental data obtained at strain stretch of 50% as per ASTM E328−13 [35]. A non-linear least square fitting was used via Abaqus to extract the coefficients of the Prony series function in Eq. (2) as shown in Figure 2 [36]:

$$g(t) = 1 - \sum_{i=1}^{N} \bar{g}_i(1 - e^{-t/\tau_i}) \quad (2)$$

Where,
g(t) = Dimensionless Relaxation Modulus.
$\bar{g}_i$, τ_i and N = Material Constants.
t = Relaxation Time.

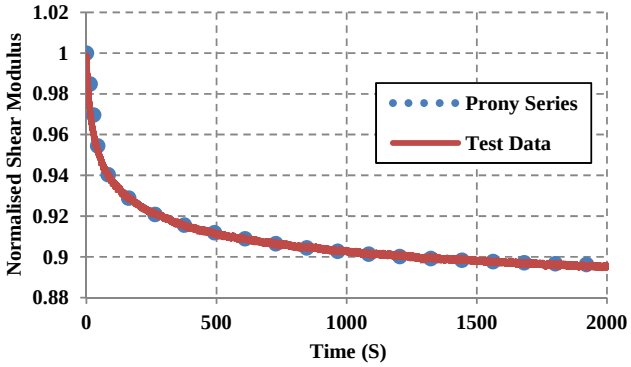

Figure 2. Fitting of Prony Series Function for Tread Sample.

The function's parameters $(\bar{g}_i, \tau_i)$ were acquired from the fitting procedure and they are as shown in Table 2:

Table 2. Function Constants of Prony Series for Tires Components.

Prony Function Constants	Tire Components		
	Tread	Sidewall	Apex
$\overline{g_1}$	0.03	0.04	0.03
τ_1	12.6	56.7	11.5
$\overline{g_2}$	0.04	0.04	0.04
τ_2	88.4	932.7	88.3
$\overline{g_3}$	0.04		0.04
τ_3	651.5		781.6

Non-Linear Viscoelasticity Property

The PRF function was adopted to represent the non-linear viscoelastic response of the tire. For non-plastic behaviour, the PRF function is made up of several response links joined with each other in parallel; a pure elastic link and a group of viscoelastic links as illustrated in Figure 3. The pure elastic link uses the hyperelastic function (i.e. Yeoh) to show the non-linear bulk elastic responses and avoid an entire stress collapse in the PRF. On the other hand, in the viscoelastic links, the deformational response in each link is divided between two components; one is elastic and the other is viscous. The elastic component in each viscoelastic link is exhibited through a scaled Yeoh function as per each link's stiffness level. As for the viscous component, the viscosity behaviour is demonstrated via the implementation of the given flow rule in Eq. (3) and "power law strain hardening" evolution law in Eq. (4) [37]:

Flow Equation:

$$D^{cr} = \frac{3}{2\bar{q}}\dot{\bar{\varepsilon}}^{cr}\bar{\sigma} = \frac{3}{2\tilde{q}}\dot{\bar{\varepsilon}}^{cr}\bar{\mathrm{T}} \qquad (3)$$

Evolution Principle:

$$\dot{\bar{\varepsilon}}^{cr} = \left(A\tilde{q}^{n}[(m+1)\bar{\varepsilon}^{cr}]^{m}\right)^{\frac{1}{m+1}} \qquad (4)$$

Where,
D^{cr} = Symmetric Portion of Velocity Gradient.
$\bar{q}$ = Equivalent Deviatoric Cauchy Stress.
$\bar{\sigma}$ = Deviatoric Cauchy Stress.
$\tilde{q}$ = Equivalent Deviatoric Kirchhoff Stress.
$\bar{\mathrm{T}}$ = Deviatoric Kirchhoff Stress.
A, m and n = Material Coefficients.
$\dot{\bar{\varepsilon}}^{cr}$ = Equivalent Creep Strain Rate.
$\bar{\varepsilon}^{cr}$ = Equivalent Creep Strain.

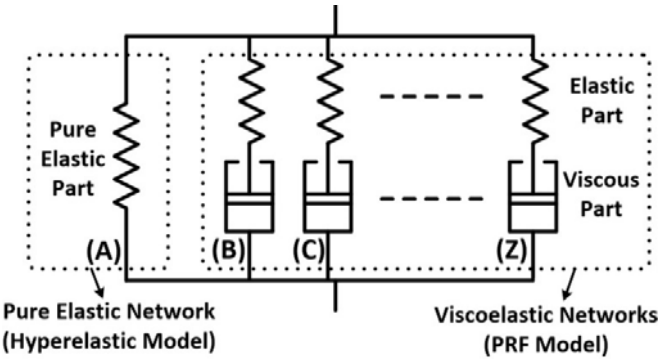

Figure 3. PRF Model Concept.

To represent the tire's non-linear viscoelasticity, the PRF function's coefficients in Eq. (4) were computed and fitted in comparison to the experimental stress relaxation results of the tire's rubbery components for various strains to account for non-linearity. This was done through creating and running the Isight 5.9 optimization model illustrated in Figure 4 [38, 39]. The Isight model included three components to compute the PRF coefficients. An Abaqus solver was used to run an FE model of rubber samples subjected to stress relaxation test at different strains similar to that done experimentally in which FE stress relaxation results were obtained. Using a data matcher, the FE relaxation outputs were compared against the experimental relaxation data as a reference and a fitting error measure was produced. To reduce the fitting error, an optimizer was utilized to search for new Yeoh and PRF coefficients using a hooke-jeeves penalty algorithm that would give a lower fitting error. The new set of Yeoh and PRF coefficients produced by the optimizer was tested using the FE model of rubber samples in the Abaqus solver and the optimization cycle was repeated until a fitting error of zero or a negligible value was reached.

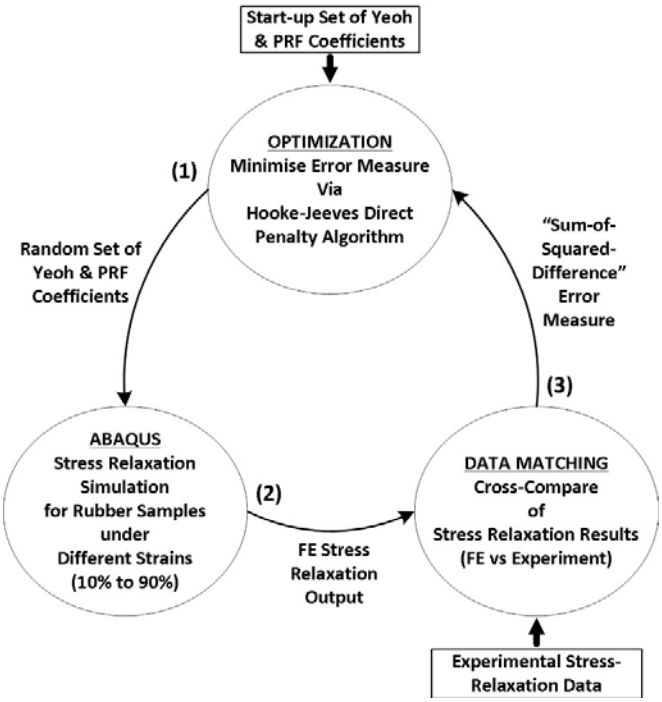

Figure 4. Isight Fitting Function.

The calibrated relevant hyperelastic and viscoelastic coefficients are shown in Table 3 with an example of Isight's data-fitting output for the tire's tread in Figure 5.

Table 3. Fitted Yeoh and PRF Coefficients for Tire Components.

		Parts		
		Tread	Sidewall	Apex
Yeoh Constants	C10	0.6	0.4	0.8
	C20	-0.07	-0.03	-0.2
	C30	0.03	0.01	0.2
PRF Constants	SR1	0.4	0.1	0.0001
	SR2	0.03	0	0.4
	SR3	0.01		0.04
	A1	3.9	0.8	0.2
	n1	4.0	2.7	1.1
	m1	-0.7	-0.1	-0.01
	A2	0.3	0.04	1.5
	n2	2.8	1.2	6.5
	m2	-0.01	-0.3	-0.4
	A3	0.4		0.05
	n3	1.2		3.1
	m3	-0.0004		-0.0004

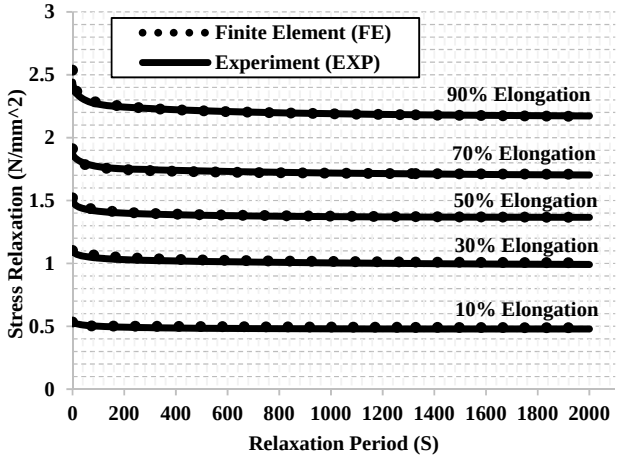

Figure 5. Time History of Stress Relaxation for Tread Sample under Different Strains by Fitted PRF Function and Experiment.

Experimental Set-up

The laboratory tire-drum rig in Figure 6 was used to conduct the experimental measurement of the tire's rolling-resistance with respect to ISO 18164:2005 [40] but at different rolling settings to address this paper's objective(s).

Figure 6. Laboratory Tire-Drum Testing Equipment.

To investigate the rolling-resistance due to the tire's internal losses (i.e. material hysteresis) only, the tire was set to roll at the straight-line and steady free-rolling settings as shown in Table 4 on a smooth, even, and hard (non-deformable) drum surface. In addition, a skim-load measurement, as per ISO 18164:2005 [40], was conducted to remove the parasitic losses including frictional losses of the tire/drum contact from the tire's rolling-resistance readings. This is to exclude the effects of acceleration, deceleration, road-surface roughness, and adhesion component of road-surface on the tire's rolling-resistance [40-44]. Furthermore, the tire had to roll at low speed of 30 Km/h in order to remove the impact of aerodynamic resistance on the rolling-resistance as well [3, 45]. This would leave the rolling-resistance measurements depending mainly on the tire's viscoelasticity (i.e. mechanical hysteresis) alone.

Table 4. Rolling Settings.

Test No	Operating Factors		
1	Velocity (Km/h)	Inflation Pressure (KPa)	Vertical Load (N)
	30	220	1000, 2000, 3000, 4000 and 5000
2	Velocity (Km/h)	Inflation Pressure (KPa)	Vertical Load (N)
	30	180, 200, 220, 240 and 260	4000

In line with this paper's scope, as indicated earlier, one of the operating conditions, the tire's rolling velocity was set fixed at 30 Km/h. This is because increasing the rolling velocity beyond 30 Km/h would cause aerodynamic-drag to form and start to gradually increase the tire rolling-resistance in which this effect escalates considerably at 120 Km/h with the formulation of standing waves in the tire [3, 27, 45, 46]. Furthermore, the rolling velocities, at and below 30 Km/h, are found to have no impact on the tire's rolling-resistance [3, 27, 46-48]. That is why the rolling velocity was set at 30 Km/h only and the material model for the FE model was tested and developed cost-effectively using strain-based (time domain) experimental data (i.e. stress-relaxation) to meet and suit the paper's scope.

Through the load cell sensor(s) of the tire-drum rig, the resistive longitudinal force at the wheel spindle was measured during tire rolling at the specified rolling settings in Table 4. From the measured force, the rolling-resistance as the energy lost from the tire's structure was calculated using Eq. (5):

$$E_{RR} = F_t \cdot \left(1 + \frac{r_L}{R}\right) \qquad (5)$$

Where,
E_{RR} = Energy Lost per Unit Travelled Distance.
F_t = Rolling-Resistance Force.
r_L = Tire Loaded Radius.
R = Wheel Drum Radius.

FE Model Set-up

To have the real tire as an FE model, a 2D axisymmetric geometry of the real tire was drawn in Abaqus/CAE, as shown in Figure 7.a, based on a cross-sectional specimen cut from the real tire. The 2D geometry had the tire's rubber and reinforcement sections located and identified while considering the tire's tread without grooves to minimise hour-glass deformations since the "grooves" have a marginal impact on the tire's rolling-resistance [26-28].

In the 2D FE model, the tire's reinforcements were created as rebar wires constructed using "SFMGAX1" surface elements and implanted inside the relevant tire rubber sections that are made up of "CGAX4R" solid elements. The reinforcements included cap plies, steel belts, body plies and beads. They were considered as istropic and linear elastic materials because they are subjected to minor and elastic strains under normal usage [31, 32]. The FE input of the reinforcement material properties was obtained by conducting the relevant experimental testing for Young moduli and referring to the related literature for poisson ratio and density [31, 32, 49-53]. Those properties are listed in Table 5 below:

Table 5. Reinforcement Properties

Reinforcement	Young Modulus (N/mm^2) × 10^3	Poission Ratio	Density (Kg/m^3) × 10^3
Cap Ply	3.4	0.3	1.3
Steel Belt	200	0.3	7.8
Body Ply	5	0.3	1.5
Bead	200	0.3	7.8

The tire's wheel rim was represented through a rigid body definition that contains and ties up the wheel centre node, the related tire/wheel contact nodes and inner rim surface (i.e. using "SFMGAX1" surface elements) facing the tire altogether. The wheel mass and rotational inertia were defined at the wheel reference node. Simplified geometry of wheel as just a surface in the tire FE model has been drawn since it is assumed non-deformable given the nature of FE simulation and to reduce the complexity of FE modelling and the needed computational resources. This is similar to Ghosh *et al.* [16], Lin and Hwang [54], Golbakhshi and Namjoo [22], Hoever [12] and Cho *et al.* [17]. Besides, the wheel part hardly plays any noticeable role in rolling-resistance simulations especially for steady-state free rolling situations [25, 26, 28, 55].

A complete 3D model of the tire was created by revolving the 2D model through 360 degrees using the procedures of "symmetric model generation" and "symmetric results transfer". The 3D tire model data were extracted into an "input" script of Abaqus and an analytical rigid (non-deformable) road drum with a straight and smooth surface was added to the model, equivalent to that used in the experiment, as shown by Figure 7.b.

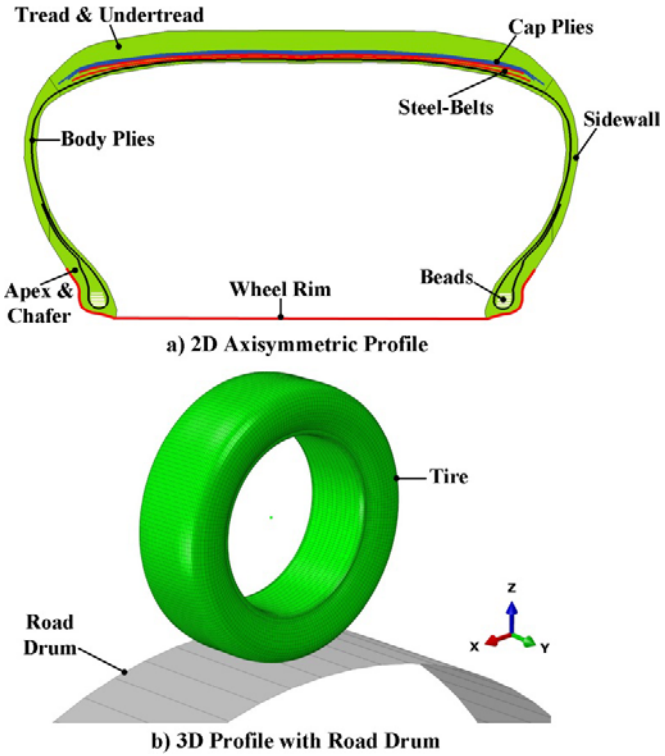

Figure 7. Two and Three Dimensional Tire FE Models.

To ensure mesh independent analysis with minimum computational resources, a mesh sensitivity check for different mesh densities of the 3D tire model was conducted in which a model with a minimum of 200 uniform mesh sectors circumferentially was found to start to provide consistent and accurate FE outputs. The end 3D model included 29600 elements for the tread, 6000 elements for the sidewall, 7400 elements for the Apex/Chafer, and 6401 elements for the wheel assembly.

FE Rolling Modelling

The previously generated "input" script was modified to include the simulation steps required to roll the tire at the testing conditions equivalent to that of the experimental work. Two job scripts were produced for the tire rolling; one utilizes the Prony series function and the other uses the PRF function. In those scripts, a general contact algorithm was used to represent the non-linear and complicated contact interaction between the tire and the road drum with a coulomb (constant) friction coefficient of 0.75 (i.e. due to free-rolling) to replicate that of the experiment [56-59].

Using the Prony series, several simulation steps and analysis tools were used to roll the tire. With Abaqus/Standard, two general static steps were made; the first was to inflate the tire and the second was to initiate tire/drum contact and then load the tire against the drum vertically. Third, a transport step was developed to roll the tire at steady-state by rolling the drum at the given angular velocity. Afterwards, the FE modelling outputs of the tire rolling in Abaqus/Standard were imported to Abaqus/Explicit to keep rolling the tire at the same rolling conditions but in a dynamic manner similar to the physical test using a dynamic rolling step to account for the dynamical and viscoelastic effects more effectively.

Using the PRF option, the modelling of tire rolling was done entirely through Abaqus/Explicit alone because the PRF function is not yet supported in the steady-state transport and the import procedures in Abaqus/Standard. Three dynamic steps were applied to perform the tire rolling. To minimize the unrequired viscoelastic impact, in the 1st and 2nd steps consecutively, the tire was inflated and after that loaded straight down against the road drum in a quasi-static manner. The 3rd step was used to free-roll the tire in a straight path by turning the road drum at the targeted constant angular velocity. In the 3rd step, a unitless damping constant of 0.03 as a portion of the tire critical damping, computed internally by Abaqus/Explicit at the contact interface, was applied in the tire/drum contact definition to reduce the noises in the FE output results [60].

Rolling-Resistance Estimation

For this study, the rolling-resistance is estimated in terms of the "energy loss per unit distance travelled" because it provides a broader description and validity. For straight free-rolling cases, this study suggests an efficient computational approach for estimating the core rolling-resistance due to the tire's internal losses, from the FE simulation outcomes, in terms of the hysteresis damping coefficient and the work transfer undergone by the tire when it deforms at its footprint as a result of being vertically loaded during rolling. The developed 3D FE model, in Figure 7, captures the complete tire's construction in great detail similar to that of the actual tire tested experimentally. As shown in Figure 8, after the tire starts to free-roll at steady-state, the hysteresis damping constant is specified from the slope of the relationship between the tire's dissipated energy (ALLCD) and its total strain energy (ALLIE) obtained from FE time history outputs. The ALLCD/ALLIE ratio covers the energy dissipation that occurs in the entire tire structure, including the footprint region, due to hysteresis damping as a result of tire deformation during rolling. This involves any deformational changes that occur to the tire's geometry or dimensional profile, such as outer-diameter, during rolling. However, the ALLCD/ALLIE ratio excludes the road drum.

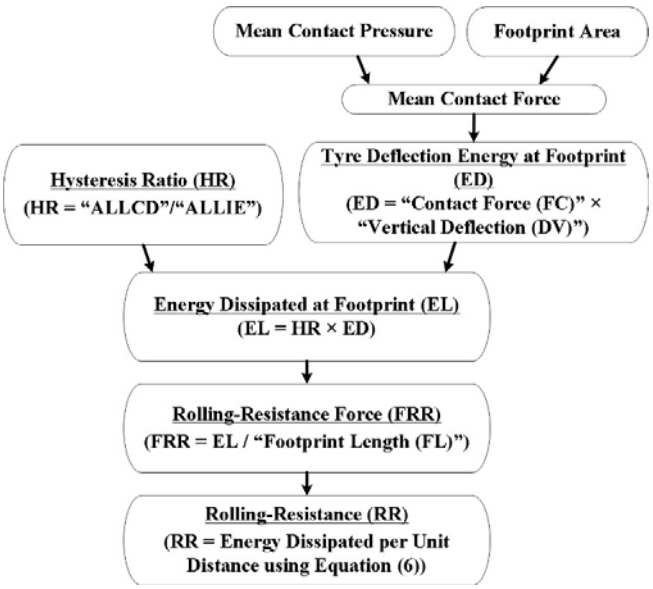

Figure 8. Rolling-Resistance Estimation Method.

Under vertical loading, the energy used to deflect the tire vertically (i.e. deflection energy (ED)) at the footprint is found from multiplying the mean of the normal contact force (FC) generated at the tire's footprint by the induced vertical deflection of the tire (DV) which are interrelated to the tire's outer-diameter [3, 61]. To determine how much energy is lost from the tire deflection energy as unrecoverable at the footprint, the tire deflection energy (ED) is multiplied by the hysteresis constant (HR) to specify the tire's energy lost at the contact region (EL). This is since the tire deformation at the contact-patch is the only significant deformation that takes place in the tire structure in which it can contribute up to 90-95% of the tire's total rolling-resistance under straight free-rolling on flat surfaces [62]. Accordingly, by taking the quotient of the energy lost from the tire at the footprint (EL) over the footprint length (FL), the tire's rolling-resistance force (FRR) can be calculated. Using Eq. (6), for flat road contact at equivalent rolling settings, it is possible to calculate the tire's rolling-resistance (RR), in the form of energy lost per unit distance travelled, from the rolling-resistance force (FRR) acquired earlier for any moved distance [40]:

$$RR = FRR \times DT \qquad (6)$$

Where,
RR = Energy Lost per Unit Distance.
FRR = Rolling-Resistance Force.
DT = Distance Travelled.

Alternatively, for tire/drum contact, Eq. (5) can be used to calculate the rolling-resistance as the energy consumed per unit distance travelled.

Results and Discussion

Rolling-Resistance

To ensure the FE model is working properly and producing the right results, for Prony series and PRF cases, the total energy balance of the tire FE model was assessed and observed to yield nearly constant output confirming that the model is following the "conservation of energy" law. Furthermore, the artificial strain energy of the tire FE model was compared to that of the model's internal energy and noted to equate to approximately 6% of the model's total strain energy. This has illustrated that the model has marginal hour-glass modes and is able to physically simulate the tire rolling correctly.

For Prony series and PRF cases, Figures 9 and 10 show the tire rolling-resistance outcomes under different rolling settings for both FE and experiment. The PRF option showed a close match and prediction of the tire's rolling-resistance with that of the physical experiment whereas Prony series provided irrationally infinitesimal output of the rolling-resistance. In this respect, tire rolling is found to be a highly non-linear process in FE modelling from the perspective of the tire's structure, contact settings, and material response, agreeing with Li *et al.* [63]. Obviously, the significant dissimilarity in the rolling-resistance results between the FE models is due to the material model chosen and its representation of the viscoelasticity since both tire FE models have the same characteristics with respect to the tire geometry and contact set-up with the exception of the employed material function (i.e. Prony series and PRF).

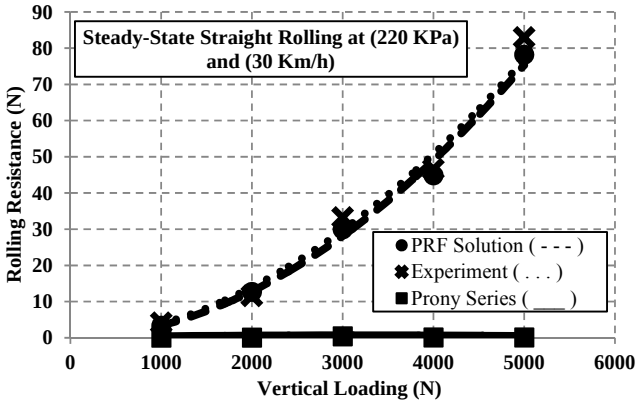

Figure 9. Relationship of Rolling-Resistance against Vertical Load.

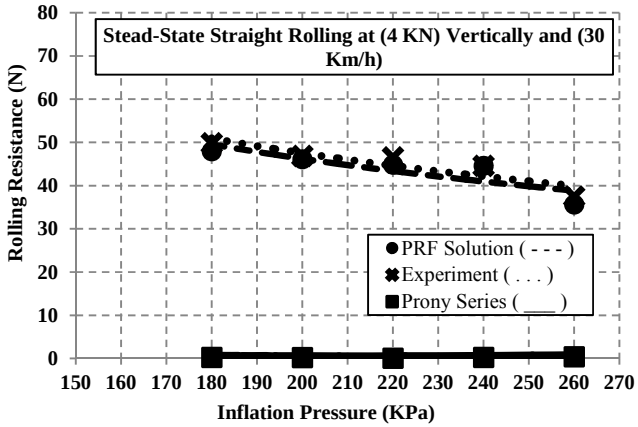

Figure 10. Relationship of Rolling-Resistance against Inflation Pressure.

For the Prony series case, the FE outputs showed unrealistic values of the tire's energy losses regardless of the various rolling settings involved as indicated in the example in Figure 11 on the contribution of the different tire parts to the total energy lost during rolling. Such outputs illustrate that the Prony series choice is unable to address the tire's non-linearity across changeable levels of loading and resultant strain when estimating the tire's energy loss and hence rolling-resistance during rolling.

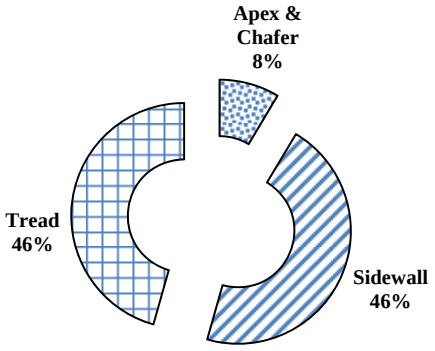

Figure 11. Energy Losses (ALLCD) as per Tire Component for Straight Free-Rolling Case at 5KN vertical load, 220KPa, and 30Km/h using Prony Solution.

The Prony function represents the tire's viscoelasticity based on the assumption that the elastic modulus is independent of the stress-strain outputs as a linear relationship is presumed. This assumption is more suited for typical materials where the induced strains in the tire are tiny or occur at a really slow rate in a way that would cause only marginal changes to the molecules set-up compared to its equilibrium setting. Dealy and Wissbrun [64] had the same conclusions. On the contrary, in reality, tire rolling promotes medium to high strain levels that occur at a fast and continuous rate leading to large complicated and non-linear molecular dislocations and shifts in the tire's structure especially the rubber components. Such a contradiction clarifies why the Prony function is being almost irresponsive to the different tire rolling settings when predicting the tire's energy losses.

However, Prony series has the potential to still be able to estimate the tire's viscoelasticity for a given limited scope in the case where a sufficient number of Prony constants is employed or if the Prony

function could be fitted to the specific rolling setting that is of interest with no other settings being involved. Such an option may be challenging and expensive to achieve depending on the complexity of the given rolling process and the diversity of the contact settings involved as agreed by Pelayo *et al.* [65].

With the PRF solution, more logical FE outcomes were produced that are in agreement with the experimental data under different rolling settings in terms of vertical load and inflation pressure.

Under different vertical loadings, the PRF displayed a nearly linearly proportional relationship between the rolling-resistance and the vertical load. The increase in the vertical load applied to the tire is found to further displace the tire downward causing more deformation to the tire's structure at the contact-patch and therefore more hysteresis damping in the process as the tire rolls. Rao *et al.* [66] showed similar findings.

For various inflation pressures, the PRF showed an inversely proportional relation between the rolling-resistance and the inflation. Higher pressure would reduce the rolling-resistance as it would make the tire stiffer and less deformable, thus reducing the mechanical hysteretic damping, in turn agreeing with Hernandez *et al.* [25].

In Figure 12, as an example, the PRF illustrates a reasonable contribution of the various tire components to the total energy lost from the tire that is in line with other research findings [17, 25, 67]. Based on the PRF outputs, the tire's tread is found to be the dominant and main component to generate most of the energy dissipation and hence cause the rolling-resistance followed by small contributions from both the sidewall and the chafer/apex.

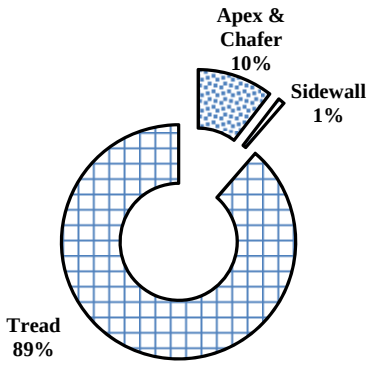

Figure 12. Energy Losses (ALLCD) as per Tire Component for Straight Free-Rolling Case at 5KN vertically, 220KPa, and 30Km/h using PRF Solution.

The accurate estimation of the actual tire's rolling-resistance provided by the PRF function is due to the function being able to successfully link the relaxation modulus to the stress-strain outputs and consider the non-linearity involved on a molecular phase across large and varied scope of strains.

Conclusion

In this study, a suggested approach to calculate the core rolling-resistance due to the tire's internal losses for straight free-rolling cases was outlined, tested and found to be correct. Furthermore, the PRF function has been proven to be more accurate and reliable than the Prony series function in accounting for the non-linear dynamic rolling of the tire when representing the tire's viscoelasticity for the FE rolling-resistance modelling. The PRF solution had a good agreement with the equivalent experimental data, whereas the Prony solution was completely out of the experimental data's scope.

The investigation outcomes indicate that the PRF option has the capability to assess and compute the rolling-resistance correctly, in particular with respect to the role of the tire's structure and the component materials used. The PRF solution devised in this study can be used by tire specialists to specifically examine the influential role of the tire's structure and material compounds adopted, as design factors, on the rolling-resistance performance of the tire for efficient tire prototype designing and development.

Nevertheless, a potential drawback in utilising the PRF function in Abaqus/Explicit is the expensive computational costs sustained which are reliant on the complexity and the scope of the FE problem at hand. To tackle such a drawback, the approach of the rolling-resistance estimation suggested in this study can be implemented, the required computational resources can be used if available, and/or mass scaling can be performed to the FE model.

The minor deviation in the rolling-resistance outputs between the PRF solution and the experimental procedure in Figures 9 and 10 may be attributed to several reasons. Such reasons could be the exclusion of the tread grooving and the reinforcement viscoelastic property from the tire FE modelling, the numerical noises produced from the usage of the FE explicit method, and the marginal non-uniformities in the actual tire construction due to the manufacturing deficiencies.

As future work, in the context of tire structural effects, the authors aim to use the current developed FE model to investigate further driving performances beside rolling-resistance such as cornering, cushioning and grip. Also, the authors look to expand the current model further to simulate and take into account other operating conditions like temperature, road roughness and aerodynamic drag.

References

1. Jae E. Data directory: future market insights on specialty silicas. Tire Technology International. 2015:70.
2. Lindemuth B. Chapter 1: An overview of tire technology. The pneumatic tire. Washington DC: National Highway Traffic Safety Administration, US department of Transportation; 2006. p. 1-27.
3. Michelin. The Tyre: Rolling Resistance and Fuel Savings. Clermont–Ferrand, France: Société de Technologie; 2003.
4. Hall DE, Moreland JC. Fundamentals of Rolling Resistance. Rubber Chemistry and Technology. 2001;74(3):525-39.
5. Redrouthu BM, Das S. Tyre modelling for rolling resistance. Göteborg, Sweden: Chalmers University of Technology; 2014.
6. Pillai PS. Effect of tyre overload and inflation pressure on rolling loss (resistance) and fuel consumption of automobile and truck/bus tyres. Indian Journal of Engineering & Materials Sciences. 2004;11:406-12.
7. Clark SK, Dodge RN. A handbook for the rolling resistance of pneumatic tires. Michigan: Industrial Development Division: Institute of Science and Technology, The University of Michigan; 1979.

8. Mavros G. Tyre models for vehicle handling analysis under steady-state and transient manoeuvres. UK: Loughborough University; 2005.
9. LaClair T. Rolling resistance. The pneumatic tire. Washington DC: US department of Transportation: National Highway Traffic Safety Administration; 2006. p. 475-532.
10. Andersen LG, Larsen JK, Fraser ES, Schmidt B, Dyre JC. Rolling resistance measurement and model development. Journal of Transportation Engineering. 2014;141(2):04014075.
11. Ghoreishy MHR. A state of the art review of the finite element modelling of rolling tyres. Iranian Polymer Journal. 2008;17(8):571-97.
12. Hoever C. The simulation of car and truck tyre vibrations, rolling resistance and rolling noise [Doctor of Philosophy]. Göteborg, Sweden: Chalmers University of Technology; 2014.
13. Andersen LG. Rolling resistance modelling: from functional data analysis to asset management system: Roskilde Universitet; 2015.
14. Ghosh S. Investigation on role of fillers on viscoelastic properties of tire tread compounds [Doctor of Philosophy]. India: Maharaja Sayajirao University of Baroda; 2011.
15. Schuring D, editor A new look at the definition of tire rolling loss. Tire Rolling Losses and Fuel Economy—An R&D Planning Workshop; 1977; Warrendale, Pennsylvania1977.
16. Ghosh P, Saha A, Mukhopadhyay R. Prediction of tyre rolling resistance using FEA. Constitutive Models for Rubber. 2003:141-6.
17. Cho J, Lee H, Jeong W, Jeong K, Kim K. Numerical estimation of rolling resistance and temperature distribution of 3-D periodic patterned tire. International Journal of Solids and Structures. 2013;50(1):86-96.
18. Luchini J, Peters J, Arthur R. Tire rolling loss computation with the finite element method. Tire Science and Technology. 1994;22(4):206-22.
19. Ebbott T, Hohman R, Jeusette J-P, Kerchman V. Tire temperature and rolling resistance prediction with finite element analysis. Tire Science and Technology. 1999;27(1):2-21.
20. Shida Z, Koishi M, Kogure T, Kabe K. A rolling resistance simulation of tires using static finite element analysis. Tire science and technology. 1999;27(2):84-105.
21. Ma G-l, Xu H, Cui W-y. Computation of rolling resistance caused by rubber hysteresis of truck radial tire. Journal of Zhejiang University-SCIENCE A. 2007;8(5):778-85.
22. Golbakhshi H, Namjoo M. An Efficient Numerical Scheme for Evaluating the Rolling Resistance of a Pneumatic Tire. International Journal of Automotive Engineering. 2015;5(2).
23. Nandi B, Dalrymple T, Yao J, Lapczyk I, editors. Importance of capturing non-linear viscoelastic material behavior in tire rolling simulations. Presented at the Meeting of the Tire Society; 2014 8-10 September 2014; USA.
24. Nyaaba W, Frimpong S, Somua-Gyimah G, Galecki G. FEA Prediction of Off-Road Tire Temperature Distribution. Science in the Age of Experience; Boston, MA: Dassault Systèmes 2016.
25. Hernandez JA, Al-Qadi IL, Ozer H. Baseline rolling resistance for tires' on-road fuel efficiency using finite element modeling. International Journal of Pavement Engineering. 2017;18(5):424-32.
26. Kim T-W, Kim H-H, Jeong H-Y, Park H-C, Kim Y-H, Choe J-H. Determination of Prony Series Parameters and Rolling Resistance Simulation of a Tire. In: Yao Z, Yuan M, Zhong W, editors. Sixth World Congress on Computational Mechanics in conjunction with the Second Asian-Pacific Congress on Computational Mechanics; Beijing, China. Beijing: Tsinghua University Press & Springer; 2004.
27. Aldhufairi HS, Olatunbosun OA. Developments in tyre design for lower rolling resistance: a state of the art review. Proceedings of the Institution of Mechanical Engineers, Part D: Journal of Automobile Engineering. 2017.
28. Wei C, Olatunbosun OA, Behroozi M. Simulation of tyre rolling resistance generated on uneven road. International journal of vehicle design. 2016;70(2):113-36.
29. Baranowski P, Malachowski J, Janiszewski J, Wekezer J. Detailed tyre FE modelling with multistage validation for dynamic analysis. Materials & Design. 2016;96:68-79.
30. Chandra S. Challenges in the Finite Element Analysis of Tire Design using ABAQUS. American Engineering Group. 2000.
31. Yang X. Finite element analysis and experimental investigation of tyre characteristics for developing strain-based intelligent tyre system [PhD]. Birmingham, UK: University of Birmingham; 2011.
32. Wei C. A finite element based approach to characterising flexible ring tire (FTire) model for extended range of operating conditions [PhD]. Birmingham, UK: University of Birmingham; 2015.
33. ASTM. D412 − 15a. Standard Test Methods for Vulcanized Rubber and Thermoplastic Elastomers—Tension. West Conshohocken, PA: ASTM International; 2016.
34. Systèmes D. Abaqus Analysis User's Guide. 2251 Hyperelastic behavior of rubberlike materials. RI, USA: Dassault Systèmes Simulia Corp.; 2013.
35. ASTM. E328 − 13 Standard Test Methods for Stress Relaxation for Materials and Structures. West Conshohocken, PA: ASTM International; 2014.
36. Systèmes D. Abaqus Analysis User's Guide. 2271 Time domain viscoelasticity. RI, USA: Dassault Systèmes Simulia Corp.; 2013.
37. Systèmes D. Abaqus Analysis User's Guide. 2282 Parallel rheological framework. RI, USA: Dassault Systèmes Simulia Corp.; 2013.
38. Obbink-Huizer C. Simuleon FEA Blog Material calibration using Abaqus (and Isight) [Internet]. 2016 [cited 2018 07 March]. Available from: https://info.simuleon.com/blog/material-calibration-using-abaqus-and-isight.
39. Connolly SJ, MacKenzie D, Comlekci T, editors. Multi-objective optimization of hyperelastic material constants: a feasibility study. 10th European Conference on Constitutive Models for Rubbers; 2017; Munich, Germany: CRC Press/Balkema.
40. ISO. ISO 18164:2005. Passenger car, truck, bus and motorcycle tyres - Methods of measuring rolling resistance. Switzerland: International Standard; 2005.
41. Hall J, Smith KL, Titus-Glover L, Wambold JC, Yager TJ, Rado Z. Guide for pavement friction. USA: Transportation Research board of the National Academies.2009. Contract No.: 108.
42. Steyn WJv, Ilse M. Evaluation of tire/surfacing/base contact stresses and texture depth. International Journal of Transportation Science and Technology. 2015;4(1):107-18.
43. Michelin. The tyre grip. Clermont–Ferrand, France: Société de Technologie Michelin 2001.
44. Henry JJ. Evaluation of pavement friction characteristics. Washington, D.C.: Transportation Research Board; 2000.
45. Katz J. Automotive aerodynamics. Wast Sussex, United Kingdom: John Wiley & Sons; 2016.
46. Thieme HvE, Dijks A, Bobo S. Measurement of tire properties. In: SK C, editor. Mechanics of Pneumatic Tires. 8. Washington D.C.: Department of Transportation; 1981. p. 541-720.
47. Bosch R. Automotive Handbook. 4 ed. Stuttgart, Germany: Bentley Publishers; 1996.

48. Clark J, Schuring D. Load, speed and inflation pressure effects on rolling loss distribution in automobile tires. Tire Science and Technology. 1988;16(2):78-95.
49. ASTM. D885/D885M − 10a (2014)E1. Standard Test Methods for Tire Cords, Tire Cord Fabrics, and Industrial Filament Yarns Made from Manufactured Organic-Base Fibers. West Conshohocken, PA: ASTM International; 2014.
50. ASTM. D2969-04. Standard Test Methods for Steel Tire Cords. West Conshohocken, PA: ASTM International; 2014.
51. Fleming RA, Livingston DI. Tire Reinforcement and Tire Performance. Philadelphia: ASTM International; 1979.
52. Smith EH. Mechanical engineer's reference book. 12th ed. Oxford, UK: Butterworth-Heinemann; 2013.
53. Engineering-Department. Materials Data Book. Cambridge, UK: Cambridge University; 2003. Available from: http://www-mdp.eng.cam.ac.uk/web/library/enginfo/cueddatabooks/materials.pdf.
54. Lin Y-J, Hwang S-J. Temperature prediction of rolling tires by computer simulation. Mathematics and Computers in Simulation. 2004;67(3):235-49.
55. Walter J. Fuel economy and effective mass: The tire's place in fuel economy. Tire Technology International. 2016;3:16.
56. Wang H, Al-Qadi IL, Stanciulescu I. Effect of surface friction on tire–pavement contact stresses during vehicle maneuvering. Journal of Engineering Mechanics. 2014;140(4):04014001.
57. Systèmes D. Abaqus Analysis User's Guide. 633 Explicit dynamic analysis. RI, USA: Dassault Systèmes Simulia Corp.; 2013.
58. Tomita H. Friction coefficients between tires and pavements surfaces. Port Hueneme, California: U. S. Naval Civil Engineering Lab.1964. Report No.: R303.
59. ADAMS M. Material Contact Properties Table. 2005. In: MSC ADAMS Help Manual [Internet]. California: MSC Software Corporation.
60. Systèmes D. Abaqus Analysis User's Guide. 3713 Contact damping. RI, USA: Dassault Systèmes Simulia Corp.; 2013.
61. Juhala M. 14 - Improving vehicle rolling resistance and aerodynamics A2 - Folkson, Richard. Alternative Fuels and Advanced Vehicle Technologies for Improved Environmental Performance: Woodhead Publishing; 2014. p. 462-75.
62. Khameneifar F, Arzanpour S, editors. Energy harvesting from pneumatic tires using piezoelectric transducers. ASME Conference Proceedings of SMASIS; 2008.
63. Li Z, Li ZR, Xia YM. An implicit to explicit FEA solving of tire F&M with detailed tread blocks. Tire Science and Technology. 2012;40(2):83-107.
64. Dealy JM, Wissbrun KF. Melt rheology and its role in plastics processing: theory and applications: Springer Science & Business Media; 2012.
65. Pelayo F, Noriega A, Lamela M-J, Fernández-Canteli A, editors. Comparison of viscoelastic moduli fitting using optimization methods. ECF19; 2012.
66. Narasimha Rao K, Kumar RK, Bohara P. A sensitivity analysis of design attributes and operating conditions on tyre operating temperatures and rolling resistance using finite element analysis. Proceedings of the Institution of Mechanical Engineers, Part D: Journal of Automobile Engineering. 2006;220(5):501-17.
67. Akutagawa K. Technology for reducing tire rolling resistance. Tribology Online. 2017;12(3):99-102.

Contact Information

Contact details for the main author should be included here. Details may include mailing address, email address, and/or telephone number (whichever is deemed appropriate).

Appendix

The Appendix is one-column. If you have an appendix in your document, you will need to insert a continuous page break and set the columns to one. If you do not have an appendix in your document, this paragraph can be ignored and the heading and section break deleted.